Journal for ImmunoTherapy of Cancer

PER2 binding to HSP90 enhances immune response against oral squamous cell carcinoma by inhibiting IKK/NF-κB pathway and PD-L1 expression

Zhiwei Zhang ,[1] Deping Sun,[2] Hong Tang,[1] Jie Ren,[3] Shilin Yin,[1] Kai Yang [1]

To cite: Zhang Z, Sun D, Tang H, *et al*. PER2 binding to HSP90 enhances immune response against oral squamous cell carcinoma by inhibiting IKK/NF-κB pathway and PD-L1 expression. *Journal for ImmunoTherapy of Cancer* 2023;**11**:e007627. doi:10.1136/jitc-2023-007627

► Additional supplemental material is published online only. To view, please visit the journal online (http://dx.doi.org/10.1136/jitc-2023-007627).

Accepted 02 October 2023

[1]Department of Oral and Maxillofacial Surgery, The First Affiliated Hospital of Chongqing Medical University, Chongqing, China
[2]Department of Otolaryngology Head and Neck Surgery, University-Town Hospital of Chongqing Medical University, Chongqing, China
[3]Department of Stomatology, The First Affiliated Hospital of Chongqing Medical University, Chongqing, China

Correspondence to
Professor Kai Yang;
cqfyyk@hotmail.com

ABSTRACT

Background Programmed death-ligand 1 (PD-L1) contributes to the immune escape of tumor cells and is a critical target for antitumor immunotherapy. However, the molecular mechanisms regulating PD-L1 expression remain unclear, hindering the development of effective therapies. Here we investigate the role and molecular mechanism of the core clock gene Period2 (PER2) in regulating PD-L1 expression and its role in the combination therapy of oral squamous cell carcinoma (OSCC).

Methods Quantitative real-time PCR, western blotting or immunohistochemistry to detect expression of PER2 and PD-L1 in OSCC tissues and cells. Overexpression and knockdown of PER2 detects the function of PER2. Bioinformatics, immunoprecipitation, GST pull-down, CHX chase assay and western blot and strip to detect the mechanism of PER2 regulation for PD-L1. A humanized immune reconstitution subcutaneous xenograft mouse model was established to investigate the combination therapy efficacy.

Results In OSCC tissues and cells, PER2 expression was reduced and PD-L1 expression was increased, the expression of PER2 was significantly negatively correlated with PD-L1. In vitro and in vivo experiments demonstrated that PER2 inhibited PD-L1 expression and enhanced T-cell-mediated OSCC cell killing by suppressing the IKK/NF-κB pathway. Mechanistically, PER2 binds to heat shock protein 90 (HSP90) through the PAS1 domain and reduces the interaction of HSP90 with inhibitors of kappa B kinase (IKKs), promoting the ubiquitination of IKKα/β and p65 nuclear translocation to inhibit IKK/NF-κB pathway, thereby suppressing PD-L1 expression. In humanized immune reconstitution subcutaneous xenograft mouse model, it was demonstrated that PER2 targeting combined with anti-PD-L1 treatment improved the inhibition of OSCC growth by promoting $CD8^+$ T-cell infiltration into the tumor.

Conclusions Our findings reveal the role and mechanism of PD-L1 regulation by PER2 and support the potential clinical application of PER2 targeting in combination with anti-PD-L1 in OSCC immunotherapy.

WHAT IS ALREADY KNOWN ON THIS TOPIC

⇒ Blocking programmed death-ligand 1 (PD-L1), an immune checkpoint on tumor cell membranes, to activate the patient's own T lymphocytes to kill tumor cells is a novel immunotherapy model, and has shown unprecedented advantages in terms of efficacy. However, the regulatory mechanism of PD-L1 expression is not clear.

WHAT THIS STUDY ADDS

⇒ We demonstrated that core clock gene Period2 (PER2) binding to heat shock protein 90 (HSP90) reduced the interaction of HSP90 with inhibitors of kappa B kinase (IKKs) and promoted ubiquitination degradation of IKKα and IKKβ, thereby inhibiting IKK/NF-κB pathway activity, p65 nuclear translocation and PD-L1 expression, while promoting $CD8^+$ T-cell infiltration in oral squamous cell carcinoma (OSCC). In the mouse tumor model, we demonstrated that PER2 targeting combined with anti-PD-L1 promoted $CD8^+$ T-cell infiltration in OSCC and improved the efficacy of OSCC immunotherapy.

HOW THIS STUDY MIGHT AFFECT RESEARCH, PRACTICE OR POLICY

⇒ The study reveals a previously unknown role of PER2 in regulating PD-L1 and antitumor immune responses and suggests that PER2 targeting in combination with anti-PD-L1 therapy is a potentially valuable new strategy to improve the efficacy of immunotherapy for OSCC.

INTRODUCTION

Oral cancer is the most common type of head and neck tumor,[1 2] and oral squamous cell carcinoma (OSCC) accounts for about 90% of oral cancer cases,[3] with an incidence that has been increasing year by year.[1 3] Although great progress has been made in treatment with surgical techniques, radiotherapy and chemotherapy, the 5-year survival rate of patients with OSCC has remained at about

50% for the past 30 years without significant improvement.[4 5] Therefore, there is an urgent need to develop new treatment strategies.

Recently, the development of tumor immunology and the breakthrough concept of treating cancer by enhancing the autoimmune system have led to a new era in cancer treatment.[6 7] In particular, immunotherapy targeting the programmed cell death 1 (PD-1) or programmed death-ligand 1 (PD-L1) immune checkpoint to block the PD-1/PD-L1 pathway, which activates the patient's own T lymphocytes to kill cancer cells, is redefining the standard of care for cancer.[7–10] Early clinical trials of PD-L1 monoclonal antibodies to block the PD-1/PD-L1 pathway for the treatment of OSCC and other head and neck tumors have shown that anti-PD-L1 therapy has the potential to prolong survival time and response duration in patients with tumor.[11–17] However, the main challenge in anti-PD-L1 therapy is the low response rate to treatment, which is effective in only a subset of patients.[18] Therefore, exploring the molecular mechanisms regulating PD-L1 and developing anti-PD-L1-based combination therapy strategies are important research directions at present.[7 18 19]

The biological clock is an endogenous timer system that controls and optimizes biological processes in the body.[20] The biological clock is an important regulator of the body's immune function and is closely related to the development of cancer.[20–22] Indeed, an abnormal biological clock has been proposed as a novel marker of cancer.[21] Period2 (PER2) is a core biological clock gene, reduced expression of which has been shown to have a key role in promoting the development of several cancers, including OSCC, head and neck squamous carcinoma, and gastric cancer.[23–26] Recent pan-cancer bioinformatics analysis showed that low expression of PER2 is correlated with PD-L1 upregulation and T-cell depletion in multiple cancers.[27] Therefore, we hypothesize that PER2 has an important regulatory effect on PD-L1 in OSCC.

The aim of this study was to investigate the role and mechanism of PD-L1 regulation by PER2 with a view to developing new combination strategies to improve the efficacy of OSCC treatment.

MATERIALS AND METHODS

Human tissue samples

OSCC paraffin tissue sections were obtained from 106 patients with OSCC hospitalized in the Department of Oral and Maxillofacial Surgery of the First Hospital of Chongqing Medical University from January 2014 to December 2016. The clinicopathological data of the patients are shown in online supplemental table S1. Sixty-two cases with paraneoplastic tissue were selected from the 106 OSCC tissue sections as controls. All patients in this study had pathologically confirmed disease and had not undergone any other treatment such as radiotherapy or chemotherapy before surgery. The majority of intermediate and advanced stage patients had additional radiotherapy or radiochemotherapy after surgery, and none of the cases had received anti-PD-L1 therapy.

Cell culture and reagents

Human normal oral epithelial (HOK) cells were purchased from Shanghai Huiying Biotechnology. TSCCA human oral squamous carcinoma cells were purchased from Shanghai Zhongqiao Xinzhou Biotechnology, and SCC15 and CAL27 human oral squamous carcinoma cells were purchased from Shanghai Tongpai Biotechnology. Short tandem repeat sequence analysis was used to identify all cell lines, and all cell lines were confirmed to be free of mycoplasma contamination. The cell culture medium consisted of fetal bovine serum (S711-001S, Lonsera, Uruguay; 10%), penicillin–streptomycin (Beyotime, China; 1%), and Dulbecco's Modified Eagle Medium (DMEM) (Gibco, USA; 89%). Cells were incubated in a thermostat (5% CO_2, 37°C).

Construction of vectors

Three short hairpin RNAs (shRNAs; PER2-RNAi#1, PER2-RNAi#2, and PER2-RNAi#3; sequences shown in online supplemental table S2) were designed and synthesized by GeneChem (Shanghai, China) to silence PER2 by targeting different sequences of the PER2 gene. The shRNA was inserted into the GV493 vector, and the plasmid was extracted and transfected into 293T cells to obtain a PER2-silencing lentivirus (sh-PER2). According to the messenger RNA (mRNA) sequence of PER2 (GenBank Accession: NM_022817), the suitable primer sequence for PCR amplification was designed and synthesized by GeneChem (Shanghai, China) (forward primer sequence: 5'-AGGTCGACTCTAGAGGATCC CGCCACCATGAA TGGATACGCGGAATTTCCGCCC-3', reverse primer sequence: 5' - ACCGTAAGT TATGTGCT AGCTTACGTCTGCTCTTCGATCCTGTGATTC-3'). The amplification products were collected, and the GV513 vector was exchanged with PER2 by BamHI/NheI digestion to construct a recombinant plasmid (OE-PER2). The plasmid was extracted and transfected into 293T cells to obtain a PER2-over-expressing lentivirus (OE-PER2).

The PER2 deletion mutation lentiviral vector was designed and synthesized by HanBio (Shanghai, China). PER2 full-length complementary DNA (cDNAs) with deletion of the PAS1, PAS2, or C terminal domains were cloned (primers shown in online supplemental table S3) and inserted into a pcDNA3.1-3xflag vector. Plasmids were extracted and transfected into 293T cells to obtain PER2 deletion mutation lentiviruses (Mut-PER2$^{\Delta PAS1}$, Mut-PER2$^{\Delta PAS2}$, and Mut-PER2$^{\Delta CT}$).

Construction of PER2 silenced, overexpressing, and mutation stable cell lines

TSCCA and SCC15 cells were infected with the PER2-overexpression lentivirus, CAL27 cells were infected with the PER2-silenced lentivirus, and TSCCA cells were infected with the PER2 deletion mutant lentiviruses. The infection efficiency was observed under a fluorescence

microscope 72 hours after infection. The cells were then screened with 2 µg/mL puromycin to obtain TSCCA and SCC15 cells with stable PER2 overexpression (OE-PER2-TSCCA and OE-PER2-SCC15), CAL27 cells with stable PER2 silencing (sh-PER2-CAL27#1, sh-PER2-CAL27#2, and sh-PER2-CAL27#3), and PER2 deletion mutant TSCCA cells (Mut-PER2$^{\Delta PAS1}$-TSCCA, Mut-PER2$^{\Delta PAS2}$-TSCCA, and Mut-PER2$^{\Delta CT}$-TSCCA). A lentivirus constructed with an empty vector without PER2 sequence was used to infect TSCCA and SCC15 cells as negative controls (NC-TSCCA and NC-SCC15), a lentivirus constructed with a scrambled plasmid was used to infect CAL27 cells as a negative control (sh-NC-CAL27). There was also a blank control group.

Immunohistochemistry

Immunohistochemistry (IHC) was performed using an SP-9000 IHC detection kit (Zhongshan Jinqiao, Beijing, China) according to the manufacturer's instructions. Paraffin sections of 4 µm thickness were routinely processed and incubated with PER2, PD-L1, p-IKKα/β, p-p65, or CD8 primary antibodies overnight at 4°C. Details of the antibodies used are provided in online supplemental table S4. The sections were then incubated with goat anti-rabbit IgG secondary antibody at room temperature for 2 hour. Then, the sections were incubated with streptavidin peroxidase for 15 min at room temperature, followed by development with diaminobenzidine (DAB). The sections were then dehydrated and sealed with neutral gel. Phosphate-buffered saline (PBS) was used instead of primary antibody in the negative control (NC) group. The IHC results were reviewed by double grading and semiquantitative grading.

Quantitative real-time PCR

Total RNA was extracted following the TaKaRa RNAiso Plus (9180, TaKaRa, Japan) instruction manual. The purity and concentration of total RNA were measured by microscopic spectrophotometry (NanoPhotometer, Implen, Germany). Total RNA was reverse transcribed into the corresponding cDNA using a PrimeScript RT Reagent Kit with gDNA Eraser (Perfect Real Time) (RR047A, TaKaRa, Japan) with the following conditions: 37°C for 15 min, 85°C for 5 s, and 4°C constant temperature. PCR primers for PER2, PD-L1, HSP90, CHUK, IKBKB, and β-actin were designed using the Oligo V.7.0 software; the primer sequences are shown in online supplemental table S5. Quantitative real-time PCR (RT-qPCR) reactions were performed in a C-1000TM thermal cycler (Bio-Rad, California, USA) according to the TB Green Premix Ex Taq (Tli RNaseH Plus, RR820A, TaKaRa) instructions. The reaction conditions were as follows: 95°C for 1.5 min, 95°C for 10 s, 60°C for 30 s, and 40 cycles. Three replicate wells were set up for each sample. The relative expression of mRNA of target gene was calculated by the $2^{-\Delta\Delta Ct}$ method using β-actin as a reference.

Co-immunoprecipitation

For each group of cell lysates, 1 µg of IgG, PER2, HSP90, IKKα, or IKKβ antibodies diluted at 1:100 was added to the cells, followed by incubation overnight at 4°C. The details of the antibodies are shown in online supplemental table S4. An appropriate amount of TBS was added to 10 µl of beads to wash them by blowing; this was repeated three times. Then, 10 µl washed protein A/G beads were added to TSCCA cell lysate that had been incubated with antibody overnight, followed by incubation at 4°C for 3 hours. The mixture was placed on a magnetic stand for 10 s, and the supernatant was aspirated. Then, 500 µl of cell lysate was vortex washed for 30 s and placed on a magnetic stand for another 10 s, and the supernatant was aspirated again; this was repeated three times. The beads and the appropriate amount of protein lysate were retained, resuspended, and mixed with 50 µl of 1×sodium dodecyl sulfate (SDS) loading buffer, boiled for 5 min at 95°C, and then subjected to western blotting.

GST pull-down assay

The plasmid containing the glutathione-S-transferase (GST)-PER2 sequence was transformed into *Escherichia coli*, and protein expression was induced with Isopropyl β-D-Thiogalactosi (IPTG). Afterwards, GST pull-down assays were performed according to the operating instructions of the Pierce GST Protein Interaction Pull-Down Kit (21516, Thermo Fisher, USA). Bacterial lysates were incubated with glutathione agarose at 4°C for 1 hour to obtain the GST-PER2 fusion protein. The GST-PER2 fusion protein was incubated with the protein to be bound in vitro, followed by elution of GST-PER2 and the bound protein with glutathione elution buffer, and then western blotting assay.

Animals and human peripheral blood mononuclear cells humanized immune reconstitution subcutaneous xenograft mouse model

Male Nod-scid mice (weight: 19–21 g; age: 6–7 weeks) were purchased from Chongqing Ensiweier Biotechnology and housed in the Laboratory Animal Center of Chongqing Medical University under specific-pathogen-free conditions. All mice were housed in fixed cages until the end of the experiment. For the tumorigenesis experiments, mice were randomly divided into three groups (n=5 per group) by a random number table method, and then each group was housed in a cage. This sample size was determined on the basis of empirical data from pilot or previous experiments. In the NC group, a suspension of NC-TSCCA cells in PBS (0·2 mL, 5×10^6 cells/mL) was injected subcutaneously (s.c.) into the left back of mice on day 0. In the NC+hPBMC group, human peripheral blood mononuclear cells (hPBMC) (1 mL, 1×10^7 cells/mL) were injected into the tail vein (intravenously (i.v.)) on day 0, followed by s.c. injection of an NC-TSCCA cell PBS suspension (0·2 mL, 5×10^6 cells/mL) into the left back. In the OE-PER2+hPBMC group, hPBMC (1 mL, 1×10^7 cells/mL; i.v.) were injected into the tail vein on day 0, followed by an OE-PER2-TSCCA cell PBS suspension (0·2 mL, 5×10^6 cells/mL; s.c.) into the left back. On day 8, significant tumor formation was observed, and on

day 20, the mice were sacrificed by cervical dislocation and tumors were removed.

For the tumor therapy experiments, on day 0, hPBMC (1 mL, 1×10^7 cells/mL; i.v.) was injected into the tail vein, followed by a TSCCA cell PBS suspension (0·2 mL, 5×10^6 cells/mL; s.c.) into the left back of the mice. Treatment was started at day 11 (when all tumor volumes had reached 50 mm^3 or more). Mice were randomly divided into four groups (n=5 per group) by a random number table method, and then each group was housed in a cage. The control group was the untreated TSCCA group (blank). Mice in the LV-OE-PER2 treatment group were treated with LV-OE-PER2 by intratumor multipoint injection (0·1 mL each) once every 3 days, four times. The durvalumab treatment group was treated with PD-L1 monoclonal antibody durvalumab (5 mg/kg) by intraperitoneal injection (i.p.) two times a week (Monday and Thursday) for 2 weeks. The LV-OE-PER2 + durvalumab combination treatment group received treatment as above. Mice were sacrificed by cervical dislocation on day 26, and tumors were harvested. All tumors harvested in the above experiments were weighed on an electronic balance; the maximum longest diameter (a) and the minimum shortest diameter (b) of the tumors were measured with vernier calipers, and tumor volume (V) was calculated using the formula $V=o.5\times a\times b^2$. The tumor tissues were then used for subsequent experimental assays. ZZ and SY were aware of the groupings during the allocation, the conduct of the experiment. JR was aware of group assignments during the outcome assessment, and the data analysis.

Other methods are shown in online supplemental materials and methods.

Statistical analysis

GraphPad Prism V.9.0 (GraphPad Software, La Jolla, California, USA) was used for data processing and statistical analysis. The results of experimental data from three independent replicates are presented as mean±SD. X^2 test was used to analyze the relationship between PER2 expression levels and clinicopathological parameters. Log-rank test was used to analyze survival differences between groups with high and low PER2 expression, and Kaplan-Meier survival curves were plotted. The Pearson method was used for correlation analyses. Student's t-test was used for comparisons between two independent sample groups, one-way analysis of variance (ANOVA) was used for one-way comparisons among multiple groups, and two-way ANOVA was used for two-factor comparisons among multiple groups. P value<0.05 was considered to indicate statistical significance.

RESULTS

Expression of PER2 and PD-L1 in OSCC and analysis of clinical significance

First, the PER2 and PD-L1 expression in the tumors of patients with OSCC was examined. IHC results showed that the expression of PER2 was significantly lower in OSCC tissues compared with paracancerous tissues, whereas the expression of PD-L1 was significantly higher (p<0.01), and the expression of PER2 was significantly negatively correlated with PD-L1 (p<0.01) (figure 1A). The expression level of PER2 was significantly negatively correlated with OSCC tumor size, cervical lymph node metastasis, and TNM (tumor-node-metastasis) clinical stage (p<0.05) (online supplemental table S1). According to the Kaplan-Meier survival analysis, the 5-year survival rate of patients with OSCC with low PER2 expression (40.52%) was significantly lower than that of those with high expression (59.09%) (p<0.01) (figure 1B). Multifactorial Cox regression analysis showed that the level of PER2 expression was an independent prognostic factor in patients with OSCC (p<0.01) (table 1).

We further evaluated the expression of PER2 and PD-L1 in three OSCC cell lines (TSCCA, SCC15, and CAL27). RT-qPCR and western blotting assays showed that PER2 mRNA and protein expression levels were significantly lower in all three OSCC cell lines compared with normal oral epithelial HOK cells, whereas PD-L1 mRNA and protein expression levels were significantly higher (p<0.05), and PER2 expression was negatively correlated with PD-L1 expression (p<0.01) (figure 1C,D). Flow cytometric assays showed significantly higher positive expression of PD-L1 on the membrane surfaces of all three OSCC cell lines compared with HOK cells (p<0.05) (figure 1E). All these results suggest that low expression of PER2 may play an important part in the development of OSCC, and that PER2 deficiency may enhance immune escape of OSCC cells by upregulating PD-L1.

PER2 enhances T-cell-mediated OSCC cell killing by suppressing PD-L1 expression

To explore the role of PER2 in the regulation of PD-L1 and the anti-OSCC immune response, we constructed two OSCC cell lines stably overexpressing PER2 (OE-PER2-TSCCA and OE-PER2-SCC15) and three OSCC cell lines with stable silencing of PER2 using shRNAs against three different specific targets (sh-PER2-CAL27#1, sh-PER2-CAL27#2, and sh-PER2-CAL27#3) (online supplemental figure 1A,B). The results of RT-qPCR, western blotting, and flow cytometric assays showed significant reductions in PD-L1 mRNA and protein expression levels, as well as in the positive expression rate of PD-L1 protein on the membrane surface of OSCC cells (p<0.01) in the two strains of OSCC cells overexpressing PER2 (figure 2A–C). The results of the T-cell-mediated tumor cell killing assay showed that overexpression of PER2 significantly increased T-cell-mediated killing of OSCC cells (p<0.001) (figure 2D). However, the OSCC CAL27 cells with silencing of PER2 via three specific targets showed the opposite alterations compared with the overexpression cells (p<0.05) (figure 2A–D). To further validate the above results, we performed rescue experiments. We transfected PER2-RNAi lentivirus into OE-PER2-TSCCA cells and showed that silencing of PER2 in TSCCA cells overexpressing PER2 significantly rescued

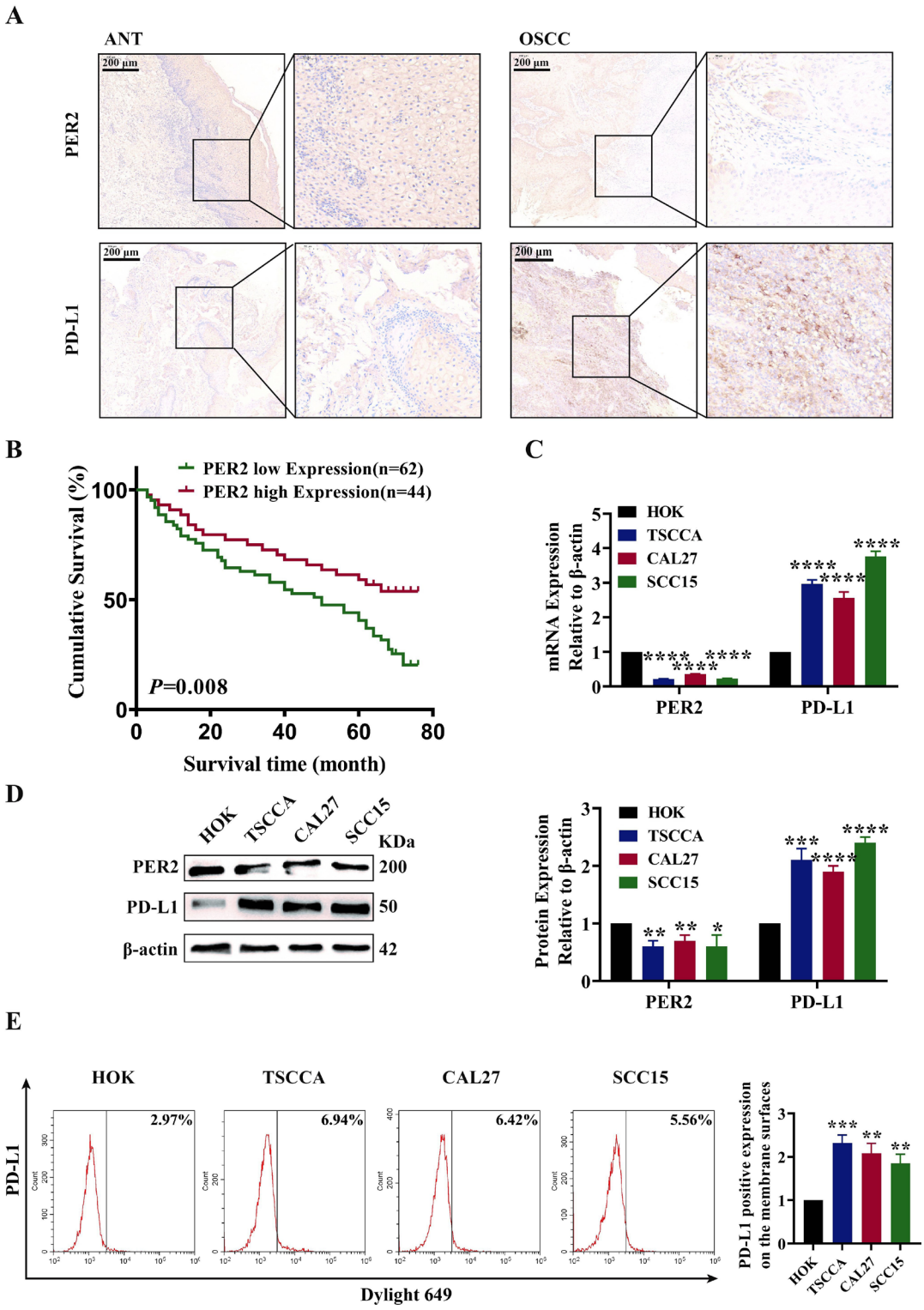

Figure 1 Expression of PER2 and PD-L1 in OSCC and analysis of clinical significance. (A) Immunohistochemical detection of PER2 and PD-L1 expression in OSCC tissues (n=106, scale bars: 200 μm), Pearson's analysis showed a negative correlation between PER2 and PD-L1 expression, R=−0.609. (B) Kaplan-Meier survival curves for patients with low and high PER2 expression (the criteria for PER2 high vs low expression is the median PER2 expression scoring). (C) Results of RT-qPCR assays to detect PER2 and PD-L1 mRNA expression in normal oral epithelial HOK cells and three OSCC cell lines (TSCCA, SCC15, and CAL27). (D) Western blotting detection of PER2 and PD-L1 protein expression in HOK cells and three OSCC cell types (TSCCA, SCC15, and CAL27), Pearson's analysis showed a negative correlation between PER2 and PD-L1 protein expression, R=−0.992. (E) Flow cytometry detection of positive PD-L1 expression on the cell membrane surfaces of HOK cells and three OSCC cell lines (TSCCA, SCC15, and CAL27). All data are representative of three independent experiments. Data are presented as mean±SD (n≥3). *, p<0.05; **, p<0.01; ***, p<0.001; ****, p<0.0001. mRNA, messenger RNA; OSCC, oral squamous cell carcinoma; PD-L1, programmed death-ligand 1; PER2, Period2 (core clock gene); RT-qPCR, quantitative real-time PCR.

Table 1 Univariate analysis and multivariate analysis of various progression in patients with OSCC Cox regression analysis

	Univariate analysis			Multivariate analysis		
	P value	HR	95% CI	P value	HR	95% CI
PER2	0.010*	0.502	0.297 to 0.850	0.005*	2.647	1.343 to 5.220
Age	0.154	1.285	0.910 to 1.814	0.828	1.051	0.673 to 1.641
Gender	0.206	0.730	0.447 to 1.190	0.125	0.659	0.387 to 1.122
Tumor differentiation	0.031*	1.400	1.031 to 1.900	0.194	1.250	0.893 to 1.749
T classification	<0.001*	12.055	6.917 to 21.011	<0.001*	8.723	4.376 to 17.387
Lymph node metastasis	<0.001*	10.879	6.036 to 19.607	0.015*	2.987	1.237 to 7.210
Clinical stage	<0.001*	7.483	4.741 to 11.810	<0.001*	3.456	1.922 to 6.213
Site	0.275	0.885	0.711 to 1.102	0.980	0.997	0.782 to 1.270

*P<0.05.
OSCC, oral squamous cell carcinoma; PER2, Period2 (core clock gene).

the reduction in PD-L1 expression in these cells, the reduction in rate of PD-L1 positive expression on the cell membrane surface, and the increase in T-cell-mediated killing of tumor cells (p<0.05) (online supplemental figure S2A–C). Furthermore, the addition of anti-PD-L1 antibody to sh-PER2-CAL27#2 cells showed that the enhanced resistance of tumor cells to T cells after PER2 knockdown was significantly rescued (online supplemental figure S2D).

For in vivo evaluation, we established an hPBMC humanized immune reconstitution subcutaneous xenograft mouse models (figure 2E). The weights and volumes of OSCC tumors were significantly lower (p<0.01) in the NC+hPBMC group (figure 2F) and levels of tumor-infiltrating $CD8^+$ T cells were significantly increased (figure 2G,H) compared with T-cell-immunodeficient Nod-scid mice (NC group). Further, in the hPBMC model with overexpression of PER2, the weights and volumes of OSCC tumors and PD-L1 expression levels were significantly lower in the OE-PER2+hPBMC group compared with the NC+hPBMC group (p<0.01) (figure 2F), whereas levels of infiltrating $CD8^+$ T cells were significantly increased in OSCC (p<0.05) (figure 2G,H). These results suggest that PER2 inhibits PD-L1 expression and enhances $CD8^+$ T-cell-mediated killing of OSCC cells, thereby inhibiting OSCC progression.

PER2 inhibits PD-L1 via the IKK/NF-κB pathway

Previous studies have demonstrated that the IKK/NF-κB pathway is a key pathway regulating PD-L1 expression in tumor cells.[28–30] We hypothesized that PER2 regulates PD-L1 expression in OSCC cells through the IKK/NF-κB pathway. We first analyzed the correlation of PER2 expression with expression of p-IKKα/β and p-p65 (key molecules in the IKK/NF-κB pathway) in tumor tissues of patients with OSCC. IHC results showed that significantly low expression of PER2 was negatively correlated with significantly high expression of p-IKKα/β and p-p65 in OSCC tissues (p<0.05) (figure 3A). Further, we verified in vitro overexpression or silencing in OSCC cells. Western blotting results showed that expression levels of p-IKKα/β, p-IκBα, p-p65, and nuclear p65 were significantly reduced in OSCC cells overexpressing PER2 (p<0.05), whereas the opposite changes occurred in OSCC cells with silenced PER2 (p<0.05) (figure 3B). These results suggest that PER2 has an important regulatory role in the IKK/NF-κB pathway. To further explore whether PER2 regulation of PD-L1 is dependent on the IKK/NF-κB pathway, we added the p65 inhibitor triptolide (PG490, MCE, USA) in sh-PER2-CAL27#2 cells for rescue assays. The results showed that the increased expression levels of PD-L1 and nuclear p65 in sh-PER2-CAL27#2 cells were significantly rescued (p<0.01) by the addition of triptolide (online supplemental figure S3A). Flow cytometric assays and T-cell-mediated tumor cell killing assays showed that the increase in positive PD-L1 protein expression on the membrane surfaces of sh-PER2-CAL27#2 cells and the decrease in T-cell-mediated OSCC cell lethality were also significantly rescued (p<0.05) by the addition of triptolide (online supplemental figure S3B,C). Finally, we examined the alterations in expression of the above molecules in subcutaneous xenografts of hPBMC mice. Western blotting assays showed that the expression levels of p-IKKα/β, p-IκBα, and nuclear p65 were significantly lower in the OE-PER2+hPBMC group compared with the NC+hPBMC group (p<0.0001) (figure 3C). Taken together, these results suggest that PER2 overexpression inhibits p65 nuclear translocation in OSCC and that PER2 regulates PD-L1 expression in a manner dependent on the IKK/NF-κB pathway.

PER2, HSP90, and IKKs form PER2/HSP90/IKKs complexes

To explore the specific mechanism by which PER2 regulates the IKK/NF-κB pathway, we downloaded the IPX0001310001 and PXD012068 protein spectrum data sets with PER2 as the decoy protein from the iProx database and the PRIDE database,[31 32] respectively. Taking the intersection of the two data sets revealed 15 candidates for possible binding to PER2 (online supplemental figure S4 and table S6). Two subunits of the HSP90 protein,

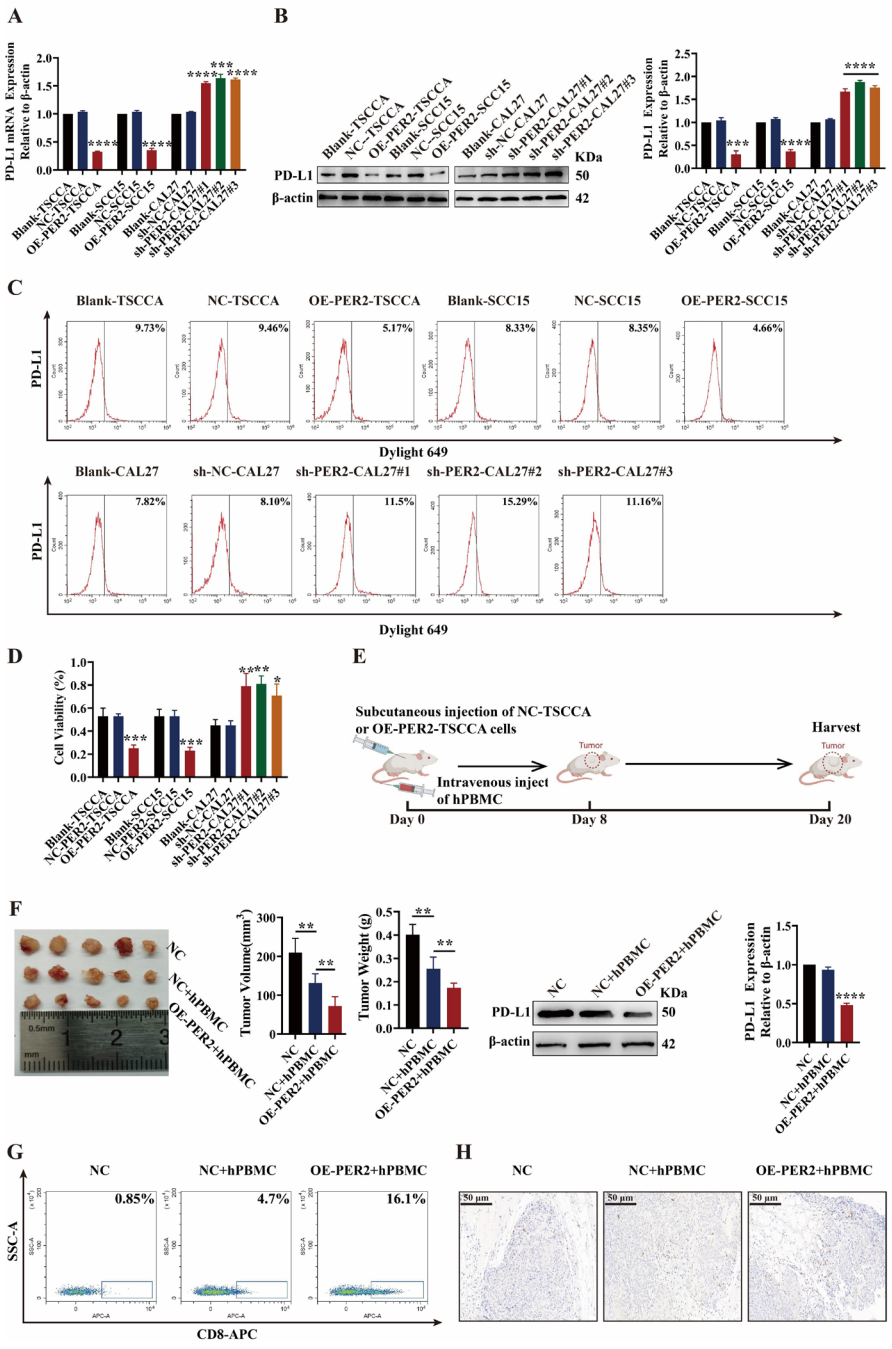

Figure 2 PER2 enhances T cell-mediated OSCC cell killing by suppressing PD-L1 expression. (A) RT-qPCR detection of PD-L1 mRNA expression in OSCC cells with overexpression or silencing of PER2. (B) Western blotting detection of PD-L1 protein expression in OSCC cells with overexpression or silencing of PER2. (C) Flow cytometry detection of positive PD-L1 expression on the membrane surfaces of OSCC cells with overexpression or silencing of PER2. (D) T-cell-mediated tumor cell killing assay to detect the killing effect of T cells on OSCC cells with overexpression or silencing of PER2, to determine the effect of PER2 alteration on the immune response of OSCC cells. (E) Schematic diagram of the hPBMC humanized immune reconstitution subcutaneous xenograft mouse model: hPBMC (1 mL, 1×10^7 cells/mL) were injected into the tail veins of Nod-scid immunodeficient mice to establish a humanized immune reconstituted mouse model. Then, a PBS suspension of NC-TSCCA or OE-PER2-TSCCA cells (0.2 mL, 5×10^6 cells/mL) was injected subcutaneously according to the grouping, to establish a mouse subcutaneous OSCC model. (F) Tumor weights and volumes in the NC group, NC+hPBMC group, and OE-PER2+hPBMC group. Western blotting was performed to detect PD-L1 protein expression in tumors of the three groups. (G) Flow cytometry detection of $CD8^+$ T-cell infiltration in the NC group, NC+hPBMC group, and OE-PER2+hPBMC group. (H) Immunohistochemical detection of $CD8^+$ T-cell infiltration in the NC group, NC+hPBMC group, and OE-PER2+hPBMC group. (n=5, scale bars: 50 μm). All data are representative of three independent experiments. Data are presented as mean±SD (n≥3). *p<0.05; **p<0.01; ***p<0.001; ****p<0.0001. hPBMC, human peripheral blood mononuclear cells; mRNA, messenger RNA; NC, negative control; OSCC, oral squamous cell carcinoma; PBS, phosphate-buffered saline; PD-L1, programmed death-ligand 1; PER2, Period2 (core clock gene); RT-qPCR, quantitative real-time PCR

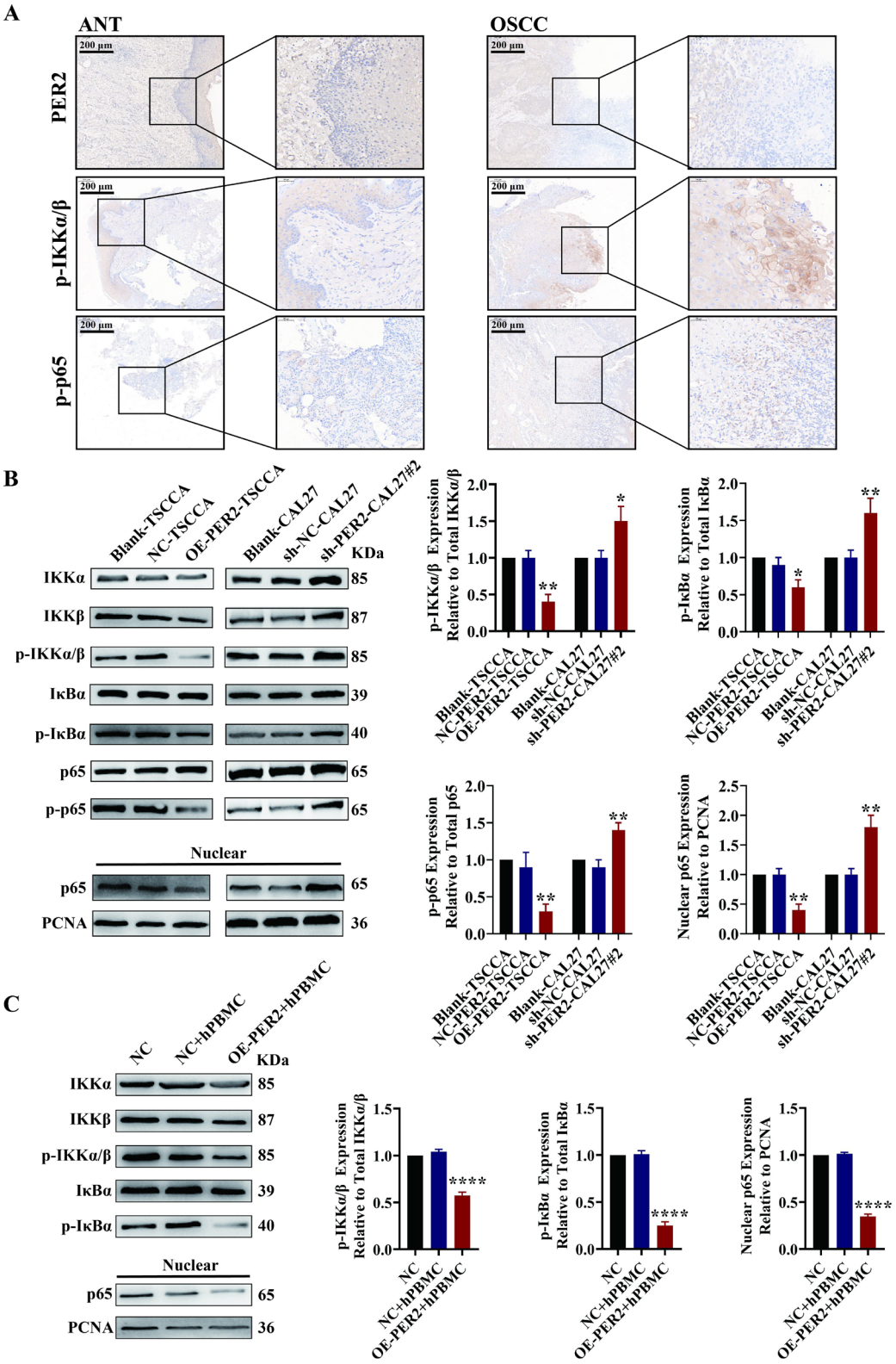

Figure 3 PER2 inhibits PD-L1 via the IKK/NF-κB pathway. (A) Immunohistochemical detection of PER2, p-IKKα/β, and p-p65 expression in OSCC tissues (n=106, scale bars: 200 μm), Pearson's analysis showed that PER2 was negatively correlated with the expression of p-IKKα/β (R=−0.577) and p-p65 (R=−0.527). (B) Western blotting to detect p-IKKα/β, p-IκBα, and p-p65 expression in OSCC cells with overexpression and silencing of PER2, as well as alterations in p65 expression in the nucleus, to examine the regulatory effect of PER2 on the IKK/NF-κB pathway. (C) Western blotting to detect the protein expression of p-IKKα/β, p-IκB, and nuclear p65 in tumors harvested from the NC group, NC+hPBMC group, and OE-PER2+hPBMC group in in vivo experiments. All data are representative of three independent experiments. Data are presented as mean±SD (n≥3). *p<0.05; **p<0.01; ***p<0.001; ****p<0.0001. NC, negative control; OSCC, oral squamous cell carcinoma; PD-L1, programmed death-ligand 1; PER2, Period2 (core clock gene).

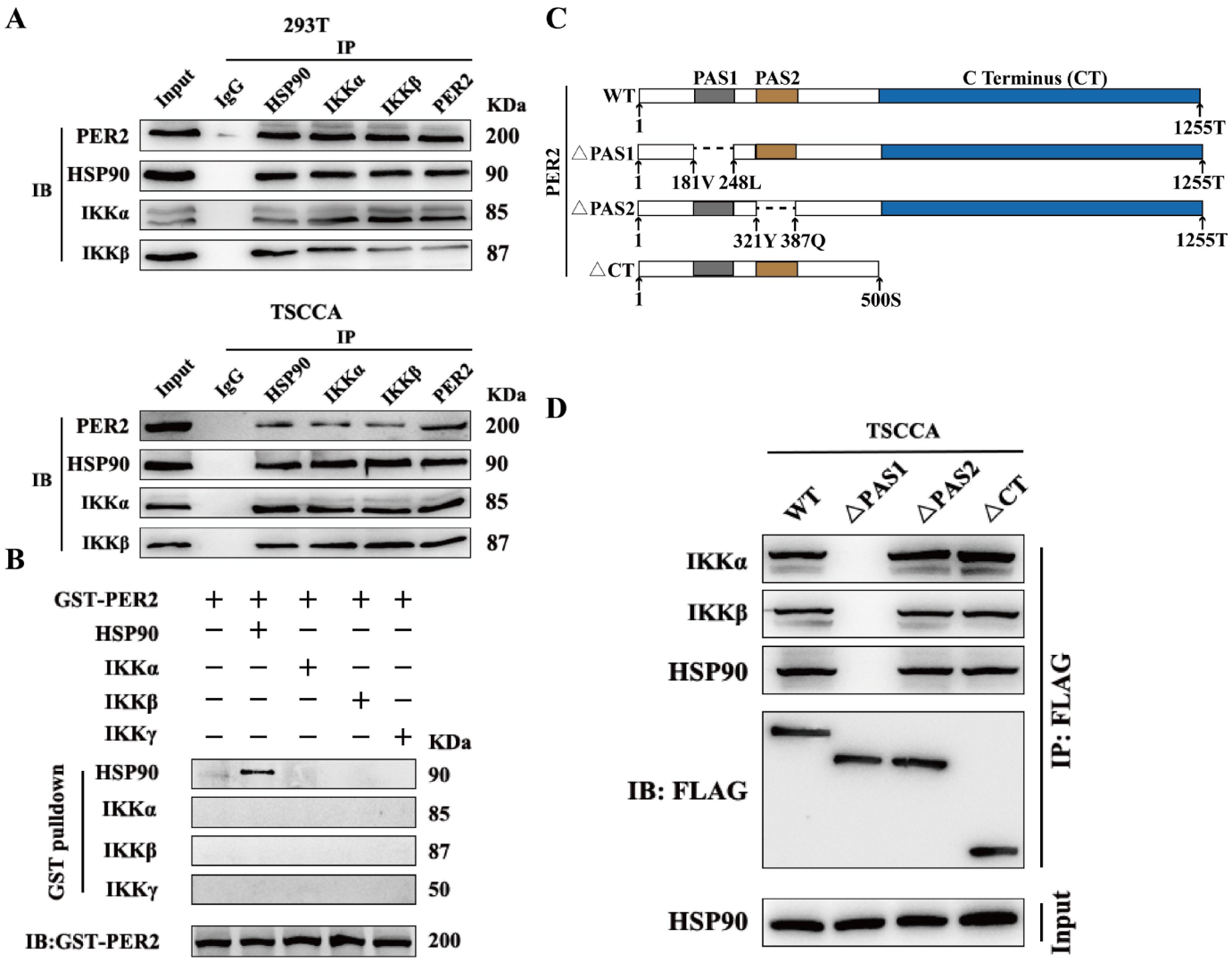

Figure 4 PER2, HSP90, and IKKs form PER2/HSP90/IKK complexes. (A) Co-IP assay to detect the binding of PER2, HSP90, IKKα, and IKKβ in 293T and TSCCA cells. (B) GST pull-down assays to detect the direct binding of PER2 to HSP90, IKKα, IKKβ, and IKKγ in vitro. (C) Construction of PER2 deletion mutant plasmids with deletion of PAS1, PAS2, and C-terminal (CT) domain, respectively. (D) Co-IP assay to detect the binding of PER2 to HSP90, IKKα and IKKβ in TSCCA cells transfected with each mutant plasmid. Co-IP, co-immunoprecipitation; PER2, Period2 (core clock gene).

HSP90α and HSP90β, were both candidates for binding to PER2; this attracted our attention because HSP90 is a molecular chaperone protein with multiple functions including maintenance of cellular protein stability.[33] HSP90 has previously been reported to interact with IKKs to form HSP90/IKK complexes, which regulate the stability of IKKα and IKKβ. Therefore, we explored whether PER2 could form a PER2/HSP90/IKK complex by interacting with HSP90. Co-immunoprecipitation (Co-IP) results showed that PER2, HSP90, and IKKs formed a PER2/HSP90/IKK complex in OSCC cells and 293T cells (figure 4A). GST pull-down results showed that PER2 could directly interact with HSP90 to form the PER2/HSP90 complex; however, it could not directly interact with IKKs (figure 4B). To further explore the domain by which PER2 binds to HSP90, we searched the UniProt (https://www.uniprot.org/) and InterPro (http://www.ebi.ac.uk/interpro/) databases and found that the main domains of PER2 involved in protein binding interactions were PAS1, PAS2, and the C-terminal domain. Therefore, we constructed three PER2 deletion mutants (Mut-PER2$^{\Delta PAS1}$-TSCCA, Mut-PER2$^{\Delta PAS2}$-TSCCA, and Mut-PER2$^{\Delta CT}$-TSCCA) with deletion of PAS1, PAS2, and the C-terminal domain, respectively (figure 4C). Co-IP assays showed the presence of the PER2/HSP90/IKK complex in Mut-PER2$^{\Delta PAS2}$-TSCCA and Mut-PER2$^{\Delta CT}$ -TSCCA cells but not in Mut-PER2$^{\Delta PAS1}$-TSCCA cells (figure 4D). The above results suggest that PER2 binds to HSP90 through the PAS1 domain to form the PER2/HSP90/IKK complex.

PER2 binding to HSP90 attenuates the interaction of HSP90 with IKKs, thereby mediating the degradation of IKKα/β ubiquitination and enhancing the immune response of OSCC

Previous studies have demonstrated that the interaction of HSP90 with IKKs reduces the degradation of IKKα and IKKβ ubiquitination and thus enhances their stability.[34 35]

We investigated whether the interaction of PER2 with HSP90 affected the interaction of HSP90 with IKKs and the ubiquitination and stability of IKKα/β. As the genes encoding IKKα and IKKβ are CHUK and IKBKB, respectively, we first examined the alterations in expression of CHUK, IKBKB, and HSP90 mRNA in OE-PER2-TSCCA cells. The RT-qPCR results showed no significant alterations in HSP90, CHUK, or IKBKB mRNA expression levels (p>0.05) in OE-PER2-TSCCA cells compared with NC-TSCCA cells (figure 5A), indicating that PER2 has no regulatory effect on HSP90, IKKα, or IKKβ at the transcriptional level. Western blotting results showed that HSP90 expression was not significantly altered in OE-PER2-TSCCA cells (p>0.05), but IKKα and IKKβ protein expression was significantly reduced (p<0.0001) (figure 5B), indicating that PER2 also failed to regulate HSP90 protein changes but could regulate changes in IKKα and IKKβ protein levels. We therefore hypothesized that PER2 interacts with HSP90 and decreases its interaction with IKKs, thereby enhancing the ubiquitinated degradation of IKKα and IKKβ. We further verified this speculation using Co-IP assays, the results of which showed a significant increase in levels of PER2/HSP90 complexes and a significant decrease in those of HSP90/IKK complexes in OE-PER2-TSCCA cells compared with NC-TSCCA cells (p<0.001) (figure 5C), suggesting that increased PER2 intercalation with HSP90 leads to decreased HSP90 intercalation with IKKs. Western blotting and strip assays and CHX tracking experiments showed that the ubiquitination levels of IKKα and IKKβ were significantly enhanced (p<0.05) in OE-PER2-TSCCA cells (figure 5D), and that the half-life of IKKα and IKKβ proteins was significantly shortened (p<0.01) (figure 5E). Western blotting results showed significant reductions in expression of PD-L1 and nuclear p65 proteins in OE-PER2-TSCCA cells (p<0.001) (figure 5C). Flow cytometry and T-cell-mediated tumor cell killing assays showed that PD-L1 protein positive expression on the membranes surface of OE-PER2-TSCCA cells was significantly reduced (p<0.05) (figure 5F), and T-cell-mediated lethality of OSCC cells was significantly increased (p<0.01) (figure 5G). However, in Mut-PER2$^{\Delta PAS1}$-TSCCA cells, all of the above indicators were significantly rescued (p<0.05) (figure 5F,G). Taken together, these results suggest that in OSCC cells, PER2 reduces the interaction of HSP90 with IKKs after interacting with HSP90 through the PAS1 domain and promotes the ubiquitinated degradation of IKKα and IKKβ, thereby inhibiting p65 nuclear translocation and PD-L1 expression and enhancing the immune response of OSCC.

PER2 targeting combined with anti-PD-L1 increases infiltration of CD8$^+$ T cells into tumors and improves the efficacy of immunotherapy

To explore the role of PER2 targeting in combination with anti-PD-L1 therapy for OSCC, we established an hPBMC humanized immune reconstitution subcutaneous xenograft mouse model that was treated with LV-OE-PER2 and durvalumab (the PD-L1 monoclonal antibody currently used clinically) in combination (figure 6A). The weights and volumes of tumors were significantly lower in the LV-OE-PER2 treatment group and the durvalumab treatment group compared with the control group (p<0.01), and significantly lower in the Lv-OE-PER2 + durvalumab treatment group than in the Lv-OE-PER2 treatment group or durvalumab treatment group (p<0.01) (figure 6B). Flow cytometry assays and IHC showed significantly increased of CD8$^+$ T-cell infiltration within tumors in the LV-OE-PER2 treatment group and in the durvalumab treatment group compared with the control group. However, CD8$^+$ T-cell infiltration within tumors were further significantly increased in the Lv-OE-PER2 + durvalumab treatment group compared with the Lv-OE-PER2 treatment group or durvalumab treatment group (p<0.05) (figure 6C,D). These results suggest that PER2 targeting or anti-PD-L1 therapy enhances CD8$^+$ T-cell-mediated killing of OSCC, and that this effect is further significantly enhanced by PER2 targeting combined with anti-PD-L1 therapy.

DISCUSSION

Blocking PD-L1, an immune checkpoint on tumor cell membranes, to activate the patient's own T lymphocytes to kill tumor cells is a novel immunotherapy model[7–10] that differs from traditional surgery, radiation, and chemotherapy and has shown unprecedented advantages in terms of efficacy.[7 8 13 14] However, the major hindrance to PD-L1-blocking therapy is the low response rate to treatment.[18] Elucidating the regulatory mechanisms of PD-L1 is key to developing combination therapy strategies with improved immune response rates and therapeutic efficacy. Currently, the regulatory mechanism of PD-L1 is receiving extensive attention.[36–41] Recent research has shown that oncogenic transcription factors including MYC, AP-1, and STAT can promote PD-L1 expression through direct binding to the PD-L1 promoter or activation of the MAPK, PTEN/PI3K/AKT, and EGFR pathways.[36 37] DNA double-strand breaks in the PD-L1 chromosomal region can activate STAT signaling via ATM/ATR/Chk1 kinase, leading to upregulation of PD-L1 expression.[38] Some non-coding RNAs, including miR-200 and miR-34a, can regulate PD-L1 expression at the post-transcriptional level by targeting the 3′ untranslated region.[39] and Shi *et al* reported that long non-coding RNA IFITM4P could upregulate PD-L1 in OSCC cells.[40] Histone acetylation and methylation of the PD-L1 promoter region can also enhance the expression of PD-L1 in cancer cells.[37] Recent studies have shown that post-translational modifications of PD-L1, such as glycosylation, phosphorylation, and ubiquitination, are important in regulating the stability of PD-L1.[37 41] Here, we identified a previously unknown role of the core biological clock gene PER2 in regulating PD-L1 expression, revealing that PER2 binds to HSP90 to suppress PD-L1 expression by inhibiting the IKK/NF-κB pathway and p65 nuclear translocation. The results of this

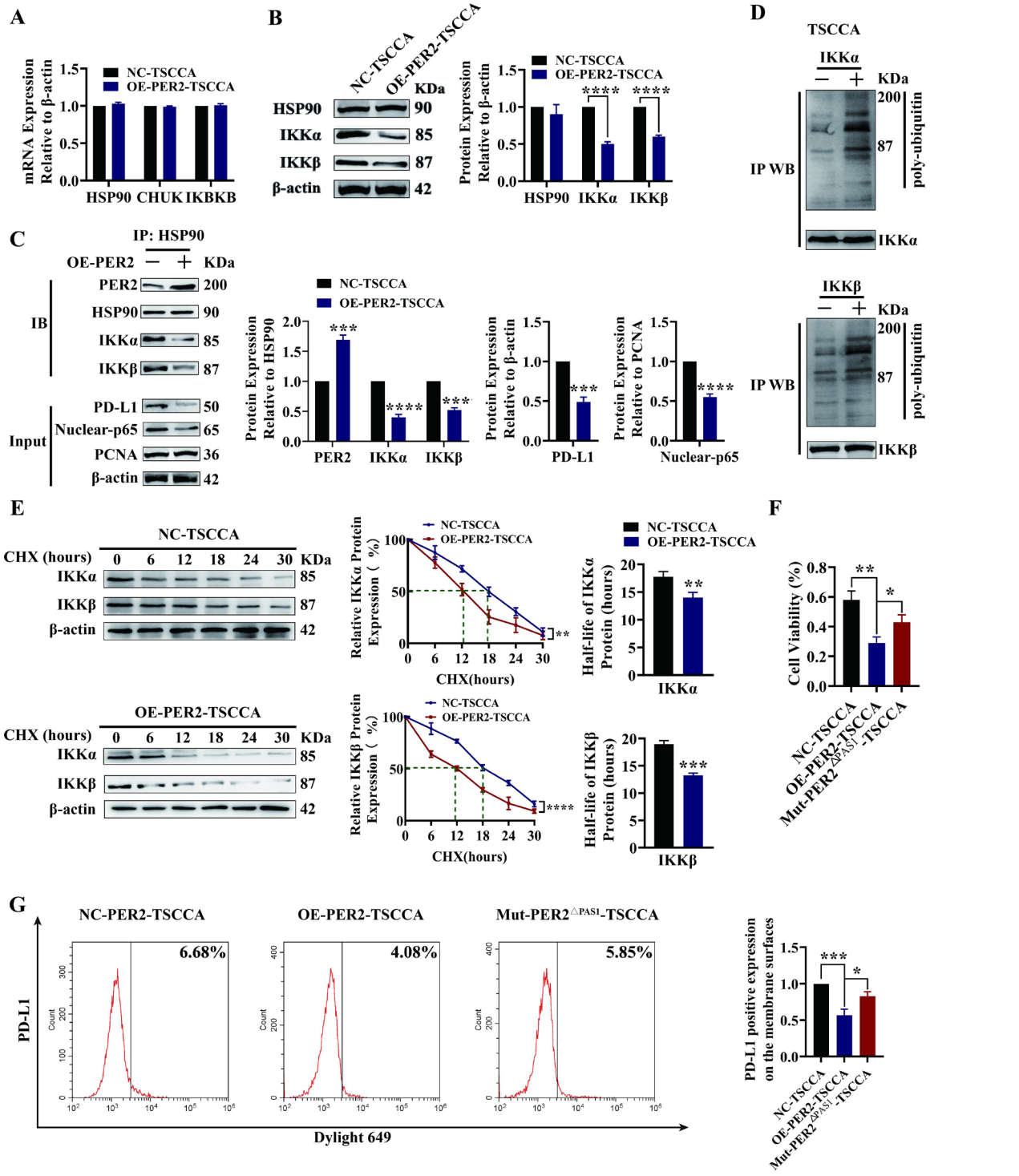

Figure 5 PER2 binding to HSP90 attenuates the interaction of HSP90 with IKKs, thereby mediating the degradation of IKKα/β ubiquitination and enhancing the immune response of OSCC. (A) RT-qPCR to detect HSP90, CHUK, and IKBKB mRNA expression in NC-TSCCA and OE-PER2-TSCCA cells. (B) Western blotting to detect the expression of HSP90, IKKα, and IKKβ proteins in NC-TSCCA and OE-PER2-TSCCA cells. (C) Co-IP combined with western blotting to detect the binding of HSP90 to PER2 and HSP90 to IKKα and IKKβ in NC-TSCCA and OE-PER2-TSCCA cells, as well as protein expression of PD-L1 and p65 in the nucleus. (D) Western blotting and strip assay to determine ubiquitination levels of IKKα and IKKβ proteins in NC-TSCCA and OE-PER2-TSCCA cells. (E) CHX chase assay to detect the half-life of IKKα and IKKβ in NC-TSCCA and OE-PER2-TSCCA cells. (F) T-cell-mediated tumor cell killing assay to detect the killing effect of T cells on NC-TSCCA, OE-PER2-TSCCA, and Mut-PER2$^{\Delta PAS1}$-TSCCA cells. (G) Flow cytometry assay to detect the protein expression of PD-L1 on the membrane surface of NC-TSCCA, OE-PER2-TSCCA, and Mut-PER2$^{\Delta PAS1}$-TSCCA cells. All data are representative of three independent experiments. Data are presented as mean±SD (n≥3). *p<0.05; **p<0.01; ***p<0.001; ****p<0.0001. Co-IP, co-immunoprecipitation; mRNA, messenger RNA; OSCC, oral squamous cell carcinoma; PD-L1, programmed death-ligand 1; PER2, Period2 (core clock gene); RT-qPCR, quantitative real-time PCR.

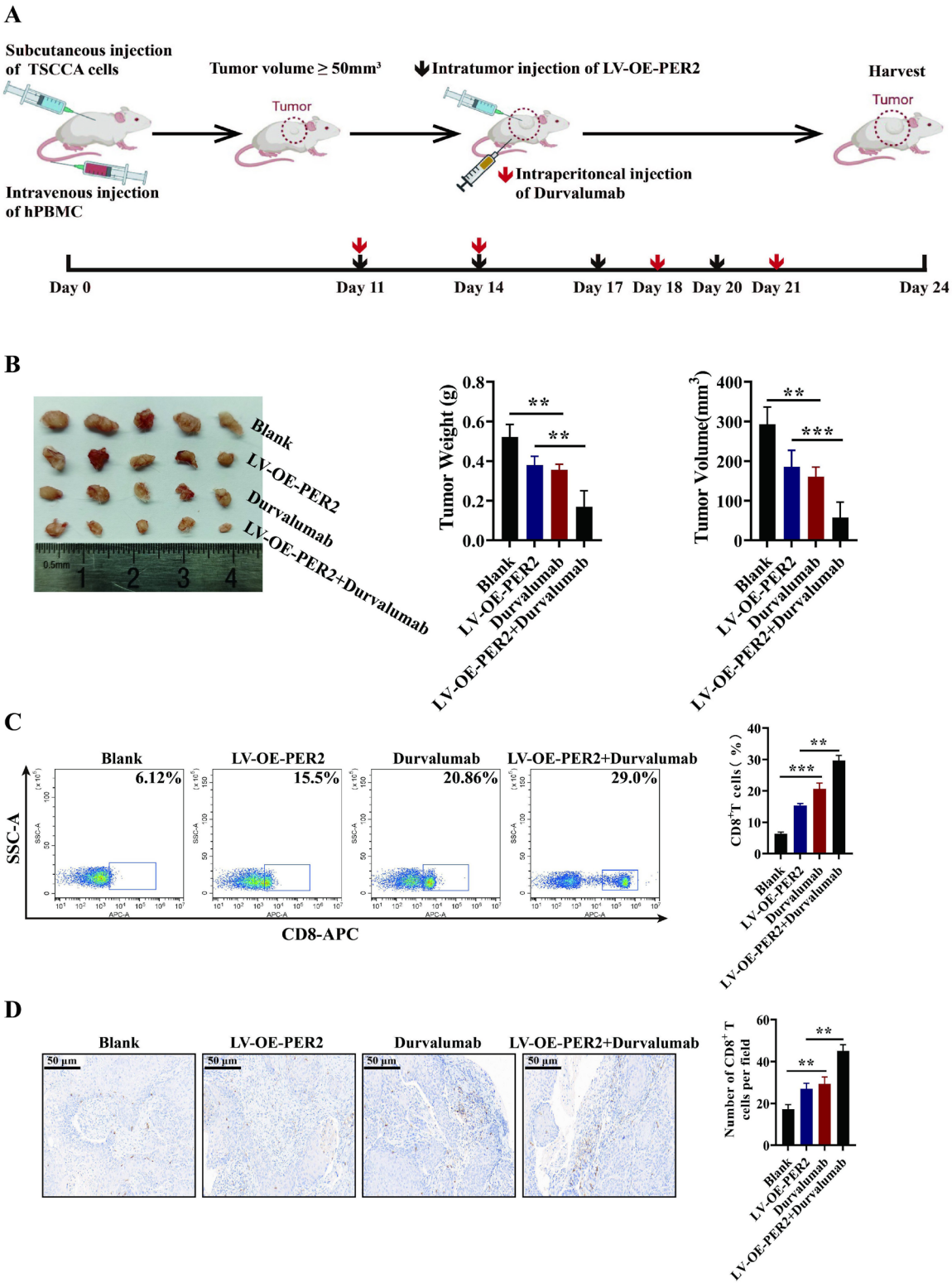

Figure 6 PER2 targeting combined with anti-PD-L1 increases the infiltration of CD8$^+$ T cells into tumors and improves the efficacy of immunotherapy. (A) Schematic diagram of the hPBMC humanized immune reconstitution mice subcutaneously injected with TSCCA cells to establish an OSCC model and post-tumorigenic treatment with LV-OE-PER2 and durvalumab. (B) Tumors were harvested at day 24, and tumor volumes and weights were measured in each group. (C) Flow cytometry to detect CD8$^+$ T-cell infiltration within the tumor in the NC group, LV-OE-PER2 group, durvalumab group, and LV-OE-PER2 + durvalumab group. (D) Immunohistochemical to detect CD8$^+$ T-cell infiltration within the tumor in the NC group, LV-OE-PER2 group, durvalumab group, and LV-OE-PER2 + durvalumab group. (n=5, scale bars: 50 μm). All data are representative of three independent experiments. Data are presented as mean±SD (n≥3). *p<0.05; **p<0.01; ***p<0.001; ****p<0.0001. hPBMC, human peripheral blood mononuclear cells; NC, negative control; OSCC, oral squamous cell carcinoma; PD-L1, programmed death-ligand 1; PER2, Period2 (core clock gene).

study extend our understanding of the regulatory mechanisms of PD-L1.

With increasing understanding of the regulatory mechanisms of PD-L1 and the different distributions and functions of PD-L1 inside and outside the cell, these findings may provide additional insight for the next generation of immune combination therapy strategies. PD-L1 is currently known to be distributed in cell membranes, intracellularly (cytoplasm and nucleus), and in the serum and has different important roles in tumor development at these different sites.[42 43] According to current knowledge, the mechanism by which anti-PD-L1 agents exert their therapeutic effect is blockade of PD-L1 on cancer cell membranes to activate T cell-mediated killing of tumor cells. This mechanism has no effect on the function of intracellular PD-L1. However, recent studies suggest that intracellular PD-L1 in cancer cells can promote tumor progression via multiple functions.[43–47] First, intracellular PD-L1 can promote cancer cell growth, metastasis, and drug resistance by participating in DNA repair pathways, activating mTOR and MAPK signaling to inhibit autophagy.[45 46] Second, with the degradation or removal of antibodies that block PD-L1 on the cancer cell membrane, intracellular PD-L1 can be transferred to the membrane surface of the cancer cell and restore its immune escape ability.[43] Third, intracellular PD-L1 can be secreted into the serum to exert inhibitory effects on T-cell activity.[37 47] For instance, Chowdhury *et al* reported that increased PD-L1 expression in the cytoplasm of papillary thyroid cancer cells significantly shortened the disease-free survival of patients.[44] Overall, results suggest that intracellular PD-L1 has important pro-cancer functions. Therefore, a combined strategy of blocking PD-L1 on cancer cell membranes and simultaneously inhibiting intracellular PD-L1 expression may represent a future research hotspot. Here, we demonstrated that a combined strategy inhibiting PD-L1 expression by overexpressing PER2 and simultaneously blocking PD-L1 on cancer cell membranes with a PD-L1 monoclonal antibody (durvalumab) could improve the efficacy of OSCC immunotherapy. However, future studies should also focus on the effects of different inhibitory approaches involving alterations in the distribution of PD-L1 within the cell as well as its translocation inside and outside the cell.

The discovery that the core clock gene PER2 inhibits PD-L1 expression also provides clues for chronopharmacology studies of anti-PD-L1-based therapeutic strategies. Current animal experiments and clinical studies have shown that selecting the optimal time of administration for drug receptors with circadian expression according to circadian rhythms can improve drug tolerance and therapeutic efficacy by 2–10-fold.[48 49] PER2 expression has been shown to have a circadian rhythm in a variety of cancer cells, including OSCC,[50 51] and Wu *et al* reported a circadian rhythm in PD-L1 promoter activity in mouse hepatocytes.[27] Although there is no direct evidence of a circadian rhythm in PD-L1 expression, our finding that PER2 has an important regulatory role in PD-L1 strongly suggests a circadian rhythm in PD-L1 expression, suggesting that chronopharmacology therapeutic strategies may be used to improve the efficacy of anti-PD-L1 treatment for tumors, which is a potentially valuable research direction.

In conclusion, we have identified a previously unknown role of PER2, a core clock gene, in mediating reduction in PD-L1 expression through inhibition of the IKK/NF-κB pathway in OSCC. Specifically, PER2 binding to HSP90 reduced the interaction of HSP90 with IKKs and promoted ubiquitinated degradation of IKKα and IKKβ, thereby inhibiting IKK/NF-κB pathway activity, p65 nuclear translocation, and PD-L1 expression while promoting $CD8^+$ T-cell infiltration in OSCC. PER2 targeting combined with an anti-PD-L1 regimen was demonstrated in a mouse tumor model to be a potentially valuable new strategy that could improve the efficacy of OSCC immunotherapy.

Contributors KY designed the study, instructed all experiments, and revised the manuscript. ZZ performed the experiments, collected the data and drafted the manuscript. DS and HT analyzed and discussed the data. JR and SY contributed to the animal models and animal analysis. All authors read, verified the underlying data and approved the manuscript. All coauthors read, edited and approved the manuscript. KY, as the guarantor, bears full responsibility for the work and/or conduct of the study, had access to the data, and controlled the decision to publish.

Funding This study was sponsored by grants from Chongqing Talents · Innovation Leading Talents Project (CQYC20200303128 to KY) and Natural Science Foundation of Chongqing, China (cstc2018jcyjAX0208 to KY).

Competing interests None declared.

Patient consent for publication Not applicable.

Ethics approval The experiment using human specimens was approved by the Biomedical Ethics Committee of the First Affiliated Hospital of Chongqing Medical University (approval number: 2021-588). All animal experiments were conducted in compliance with institutional guidelines and approved by the Biomedical Ethics Committee of the First Hospital of Chongqing Medical University (approval number: 2018-102).

Provenance and peer review Not commissioned; externally peer reviewed.

Data availability statement Data are available in a public, open access repository. All data relevant to the study are included in the article or uploaded as supplementary information.

ORCID iDs
Zhiwei Zhang http://orcid.org/0009-0005-5033-8901
Kai Yang http://orcid.org/0000-0002-0884-3534

REFERENCES

1 Siegel RL, Miller KD, Fuchs HE, *et al*. Cancer Statistics. *CA Cancer J Clin* 2022;72:7–33.

2 Sung H, Ferlay J, Siegel RL, *et al*. Global cancer Statistics 2020: GLOBOCAN estimates of incidence and mortality worldwide for 36 cancers in 185 countries. *CA Cancer J Clin* 2021;71:209–49.
3 Chi AC, Day TA, Neville BW. Oral cavity and oropharyngeal squamous cell carcinoma--an update. *CA Cancer J Clin* 2015;65:401–21.
4 Giraldi L, Leoncini E, Pastorino R, *et al*. Alcohol and cigarette consumption predict mortality in patients with head and neck cancer: a pooled analysis within the International head and neck cancer epidemiology (INHANCE) consortium. *Ann Oncol* 2017;28:2843–51.
5 Sasahira T, Kirita T. Hallmarks of cancer-related newly Prognostic factors of oral squamous cell carcinoma. *IJMS* 2018;19:2413.
6 Billan S, Kaidar-Person O, Gil Z. Treatment after progression in the era of Immunotherapy. *Lancet Oncol* 2020;21:e463–76.
7 Wang Y, Wang M, Wu H, *et al*. Advancing to the era of cancer Immunotherapy. *Cancer Communications* 2021;41:803–29. 10.1002/cac2.12178 Available: https://onlinelibrary.wiley.com/toc/25233548/41/9
8 Topalian SL, Taube JM, Pardoll DM. Neoadjuvant Checkpoint blockade for cancer Immunotherapy. *Science* 2020;367:eaax0182.
9 Cohen EEW, Bell RB, Bifulco CB, *et al*. The society for Immunotherapy of cancer consensus statement on Immunotherapy for the treatment of squamous cell carcinoma of the head and neck (HNSCC). *J Immunother Cancer* 2019;7:184.
10 Gubin MM, Vesely MD. Cancer Immunoediting in the era of Immuno-oncology. *Clinical Cancer Research* 2022;28:3917–28.
11 Darragh LB, Knitz MM, Hu J, *et al*. A phase I/IB trial and biological correlate analysis of Neoadjuvant SBRT with single-dose Durvalumab in HPV-unrelated locally advanced HNSCC. *Nat Cancer* 2022;3:1300–17.
12 Psyrri A, Fayette J, Harrington K, *et al*. Durvalumab with or without Tremelimumab versus the EXTREME regimen as first-line treatment for recurrent or metastatic squamous cell carcinoma of the head and neck: KESTREL, a randomized, open-label, phase III study. *Ann Oncol* 2023;34:262–74.
13 Zandberg DP, Algazi AP, Jimeno A, *et al*. Durvalumab for recurrent or metastatic head and neck squamous cell carcinoma: results from a single-arm, phase II study in patients with ≥25% tumour cell PD-L1 expression who have progressed on platinum-based chemotherapy. *Eur J Cancer* 2019;107:142–52.
14 Guigay J, Lee K-W, Patel MR, *et al*. Avelumab for platinum-ineligible/refractory recurrent and/or metastatic squamous cell carcinoma of the head and neck: phase IB results from the JAVELIN solid tumor trial. *J Immunother Cancer* 2021;9:e002998.
15 Siu LL, Even C, Mesía R, *et al*. Safety and efficacy of Durvalumab with or without Tremelimumab in patients with PD-L1–low/negative recurrent or metastatic HNSCC the phase 2 CONDOR randomized clinical trial. *JAMA Oncol* 2019;5:195–203.
16 Ferris RL, Haddad R, Even C, *et al*. Durvalumab with or without Tremelimumab in patients with recurrent or metastatic head and neck squamous cell carcinoma: EAGLE, a randomized, open-label phase III study. *Ann Oncol* 2020;31:942–50.
17 Colevas AD, Bahleda R, Braiteh F, *et al*. Safety and clinical activity of Atezolizumab in head and neck cancer: results from a phase I trial. *Ann Oncol* 2018;29:2247–53.
18 Cristina V, Herrera-Gómez RG, Szturz P, *et al*. Immunotherapies and future combination strategies for head and neck squamous cell carcinoma. *Int J Mol Sci* 2019;20:5399.
19 Ran X, Yang K. Inhibitors of the PD-1/PD-L1 axis for the treatment of head and neck cancer: Current status and future perspectives. *Drug Des Devel Ther* 2017;11:2007–14.
20 Zhang Z, Zeng P, Gao W, *et al*. Circadian clock: a regulator of the immunity in cancer. *Cell Commun Signal* 2021;19:37.
21 El-Athman R, Relógio A. Escaping circadian regulation: an emerging hallmark of cancer? *Cell Syst* 2018;6:266–7.
22 Cash E, Sephton S, Woolley C, *et al*. The role of the circadian clock in cancer hallmark acquisition and immune-based cancer Therapeutics. *J Exp Clin Cancer Res* 2021;40:119.
23 Xiong H, Yang Y, Yang K, *et al*. Loss of the clock gene Per2 is associated with cancer development and altered expression of important tumor-related genes in oral cancer. *Int J Oncol* 2018;52:279–87.
24 Li Y-Y, Jin F, Zhou J-J, *et al*. Downregulation of the circadian period family genes is positively correlated with poor head and neck squamous cell carcinoma prognosis. *Chronobiol Int* 2019;36:1723–32.
25 Zhao H, Zeng Z-L, Yang J, *et al*. Prognostic relevance of Period1 (Per1) and Period2 (Per2) expression in human gastric cancer. *Int J Clin Exp Pathol* 2014;7:619–30.
26 Xu B, Jiang Y. Aberrant expression of Per1, Per2 and Per3 and their Prognostic relevance in non-small cell lung cancer. *Int J Clin Exp Pathol* 2014;7:7863–71.
27 Wu Y, Tao B, Zhang T, *et al*. Pan-cancer analysis reveals disrupted circadian clock Associates with T cell exhaustion. *Front Immunol* 2019;10:2451.
28 Guo D, Tong Y, Jiang X, *et al*. Aerobic Glycolysis promotes tumor immune evasion by Hexokinase2-mediated Phosphorylation of IκBα. *Cell Metab* 2022;34:1312–24.
29 Zhou Y, Jin X, Yu H, *et al*. Hdac5 modulates PD-L1 expression and cancer immunity via P65 Deacetylation in Pancreatic cancer. *Theranostics* 2022;12:2080–94.
30 Chang H, Xu Q, Li J, *et al*. Lactate secreted by Pkm2 upregulation promotes Galectin-9-mediated immunosuppression via inhibiting NF-KB Pathwayin HNSCC. *Cell Death Dis* 2021;12:725.
31 Wu R, Dang F, Li P, *et al*. The circadian protein Period2 suppresses Mtorc1 activity via recruiting Tsc1 to Mtorc1 complex. *Cell Metabolism* 2019;29:653–667. 10.1016/j.cmet.2018.11.006 Available: https://doi.org/10.1016/j.cmet.2018.11.006
32 Brenna A, Olejniczak I, Chavan R, *et al*. Data from: Cyclin-dependent kinase 5 (Cdk5) regulates the circadian clock. *eLife* 2019;8. 10.7554/eLife.50925 Available: https://doi.org/10.7554/elife.50925
33 Jolly C, Morimoto RI. Role of the heat shock response and molecular Chaperones in Oncogenesis and cell death. *J Natl Cancer Inst* 2000;92:1564–72.
34 Broemer M, Krappmann D, Scheidereit C. Requirement of Hsp90 activity for Ikappab kinase (IKK) biosynthesis and for Constitutive and inducible IKK and NF-kappaB activation. *Oncogene* 2004;23:5378–86.
35 Chen G, Cao P, Goeddel DV. TNF-induced recruitment and activation of the IKK complex require Cdc37 and Hsp90. *Mol Cell* 2002;9:401–10.
36 Shen X, Zhang L, Li J, *et al*. Recent findings in the regulation of programmed death ligand 1 expression. *Front Immunol* 2019;10:1337.
37 Cha J-H, Chan L-C, Li C-W, *et al*. Mechanisms controlling PD-L1 expression in cancer. *Mol Cell* 2019;76:359–70.
38 Sato H, Niimi A, Yasuhara T, *et al*. DNA double-strand break repair pathway regulates PD-L1 expression in cancer cells. *Nat Commun* 2017;8:1751.
39 Wang Q, Lin W, Tang X, *et al*. The roles of microRNAs in regulating the expression of PD-1/PD-L1 immune Checkpoint. *IJMS* 2017;18:2540.
40 Shi L, Yang Y, Li M, *et al*. Lncrna Ifitm4P promotes immune escape by up-regulating PD-L1 via dual mechanism in oral carcinogenesis. *Mol Ther* 2022;30:1564–77.
41 Lim S-O, Li C-W, Xia W, *et al*. Deubiquitination and stabilization of PD-L1 by Csn5. *Cancer Cell* 2016;30:925–39.
42 Kornepati AVR, Vadlamudi RK, Curiel TJ. Programmed death ligand 1 signals in cancer cells. *Nat Rev Cancer* 2022;22:190:174–89.:.
43 Wu Y, Chen W, Xu ZP, *et al*. PD-L1 distribution and perspective for cancer Immunotherapy-blockade, knockdown, or inhibition. *Front Immunol* 2019;10:2022.
44 Chowdhury S, Veyhl J, Jessa F, *et al*. Programmed death-ligand 1 overexpression is a Prognostic marker for aggressive papillary thyroid cancer and its variants. *Oncotarget* 2016;7:32318–28.
45 Hanks BA. “The "inside" story on tumor-expressed PD-L1”. *Cancer Res* 2022;82:2069–71.
46 Kornepati AVR, Boyd JT, Murray CE, *et al*. Tumor intrinsic PD-L1 promotes DNA repair in distinct cancers and suppresses PARP inhibitor-induced synthetic lethality. *Cancer Res* 2022;82:2156–70.
47 Theodoraki M-N, Yerneni SS, Hoffmann TK, *et al*. Clinical significance of PD-L1$^+$ Exosomes in plasma of head and neck cancer patients. *Clin Cancer Res* 2018;24:896–905.
48 Ortiz-Tudela E, Mteyrek A, Ballesta A, *et al*. Cancer Chronotherapeutics: experimental, theoretical, and clinical aspects. *Handb Exp Pharmacol* 2013;217:261–88.
49 Lévi F, Okyar A, Dulong S, *et al*. Circadian timing in cancer treatments. *Annu Rev Pharmacol Toxicol* 2010;50:377–421. 10.1146/annurev.pharmtox.48.113006.094626 Available: https://www.annualreviews.org/toc/pharmtox/50/1
50 Tan X-M, Ye H, Yang K, *et al*. Circadian variations of clock gene Per2 and cell cycle genes in different stages of carcinogenesis in golden Hamster Buccal mucosa. *Sci Rep* 2015;5:9997.
51 Kuramoto S, Nakagawa H. A molecular mechanism regulating circadian expression of vascular endothelial growth factor in tumor cells. *Cancer Res* 2003;63:7277–83.